CIVIL ENGINEERING JOURNAL

Article no. 38

THE CIVIL ENGINEERING JOURNAL 4-2025

ANALYSIS OF THE DOWNWARD DEFLECTION PARAMETERS BEFORE AND AFTER EXTERNAL PRESTRESSING REINFORCEMENT OF CONTINUOUS RIGID FRAME BRIDGES

Jianwei Li, Wentao Xu and Hongjian Lu

Puyang Institute of Technology, Henan University, West Section of Yellow River Road, Puyang, Henan Province, China; pygxyljw@163.com

Received: *22.05.2025*
Received in revised form: *28.06.2025*
Accepted: *11.11.2025*

ABSTRACT

Due to a lack of foresight by designers during bridge planning, outdated specifications that have not been updated in a timely manner, or construction errors during the building process, bridge structures may be overloaded, ultimately leading to excessive deflection in the main span of continuous rigid frame bridges. Therefore, it is urgent to study the causes of downward deflection in continuous rigid frame bridges and explore their reinforcement methods. This paper conducts parametric analysis by using the finite element method to explore the influence degree of different factors on deflection. This paper addresses the issue of severe mid-span deflection in a specific continuous rigid frame bridge and investigates the impact of various factors, including internal prestress loss, stiffness reduction, shrinkage and creep, over-excavation (possibly referring to excessive excavation or over-dimensioning in construction), shear deformation, external prestress loss, and overloading, on the downward deflection of continuous rigid frame bridges. The study identifies the most significant factor contributing to this deflection. Upon comprehensive comparison of all factors, stiffness reduction is found to be the primary cause of mid-span deflection. When the stiffness is reduced by 10%, the deflection difference plot shows that the maximum decrease in deflection near the mid-span is 8.76mm. For reinforced bridges, external prestress loss and overloading are the most critical factors. In calculations for continuous rigid frame bridges, shear deformation cannot be neglected.

KEYWORDS

Continuous rigid frame bridge, External prestressing, Reinforcement, Downward deflection

INTRODUCTION

Continuous rigid frame bridges belong to the category of continuous beam bridges in terms of their bridge span structure system. Continuous beam bridges are an ancient type of beam structure system, known for their small deformation, high structural stiffness, smooth and comfortable ride, few expansion joints, simple maintenance, and strong earthquake resistance, which have been adopted by people for a long time [1-4]. However, due to limitations in construction methods, the span of continuous beam bridges made of concrete structures before the 1960s was less than 100m. With the emergence of cantilever pouring and cantilever assembly construction methods, T-shaped rigid frame bridges came into being. Nevertheless, this structure featured hinges

in the middle and underestimated creep and shrinkage deformations of concrete. Additionally, factors such as temperature led to obvious angular deformations at the hinged joints, which was detrimental to traffic. Therefore, the continuous beam-type rigid frame bridge, which is advantageous for traffic, emerged [5,6].

Prestressed continuous rigid frame bridges possess many advantages of both T-shaped rigid frame bridges and continuous beams. The load-bearing beams are continuous beams and are rigidly connected to the piers [7-10]. From the perspective of the important characteristics of structural mechanics, the upper structure of the continuous rigid frame system is similar to that of a continuous beam. Due to significant temperature changes, for continuous rigid frame bridges with large spans and low pier heights, concrete shrinkage often results in significant bending moments at the pier bases. As the bridge is used and operated over time, some of its potential issues gradually emerge, posing serious threats to the bridge's sustained use in the future [11,12]. In reality, beam deflection and beam cracking often occur together and are coupled.

The main defects of continuous rigid frame bridges are currently classified into the following types: cracks in the top slab, bottom slab, and mid-span web [13]. The presence of these cracks significantly reduces the performance of prestressed concrete continuous rigid frame bridges, decreases the overall stiffness of the main beam, and compromises structural quality [14]. If timely maintenance and repairs are not carried out, it will inevitably lead to damage to the main structure and even serious accidents. Excessive downward deflection in the mid-span of continuous rigid frame bridges has become a common issue. Long-term downward deflection of large-span prestressed concrete box girders is indeed a flaw in the system, and specific factors such as material and environmental differences, as well as variations in construction quality across different regions, are not inevitable causes of deflection. Only by effectively understanding and mastering the downward deflection of continuous rigid frame bridges can we truly enhance the bridge's sustained load-bearing capacity, prevent stress cracks, and effectively control the magnitude of beam deflection. Due to the relatively short service life of prestressed concrete structures, many issues have not yet been exposed [15-17]. Among them, the most common is corrosion of reinforcing steel.

Due to insufficient understanding of continuous rigid frame bridges in the early stages, some continuous rigid frame bridges both domestically and internationally have developed common defects after years of operation, such as excessive mid-span deflection and numerous cracks in the box girder. The causes of these defects may include prestress loss, stiffness reduction, overloading, or concrete creep and shrinkage [18-20]. This paper analyzes the impact of various factors on mid-span deflection based on the characteristics of severe mid-span deflection in a specific continuous rigid frame bridge. It provides references for reinforcement measures targeting mid-span deflection and other defects in this type of bridge, which is valuable for the development of bridge reinforcement technology and engineering issues related to reinforcement measures for continuous rigid frame bridges.

PROJECT OVERVIEW

A continuous rigid frame bridge is a large prestressed concrete structure. The span arrangement of the bridge is 35 m + 60 m + 90 m + 60 m + 35 m, with a total length of 280 m, situated on a 2.2% longitudinal slope. The deck’s horizontal layout consists of a 0.75 m parapet base, a 10.5m carriageway, and another 0.75 m parapet base. The pedestrian load for this bridge is 3.5 kN/m, and the design load is for Highway-20 vehicles and Trailer-120. The general layout of the bridge type is shown in Figure 1. The cross-sections at the mid-span and pier top of the box girder are illustrated in Figure 2.

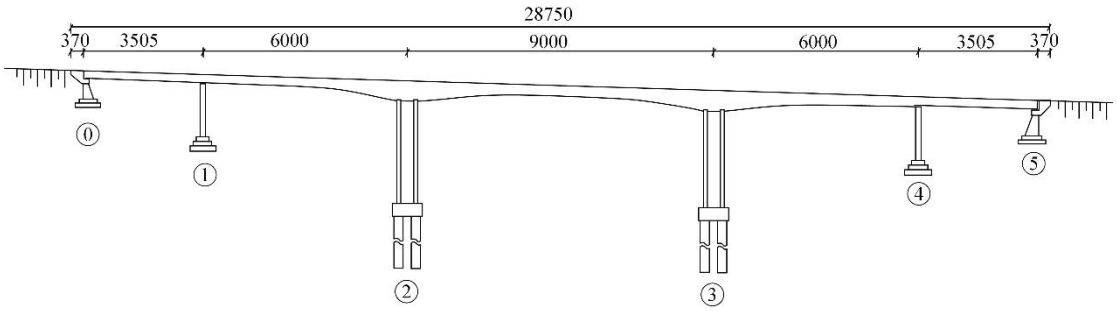

Fig.1 - General layout of bridge type (Unit: cm)

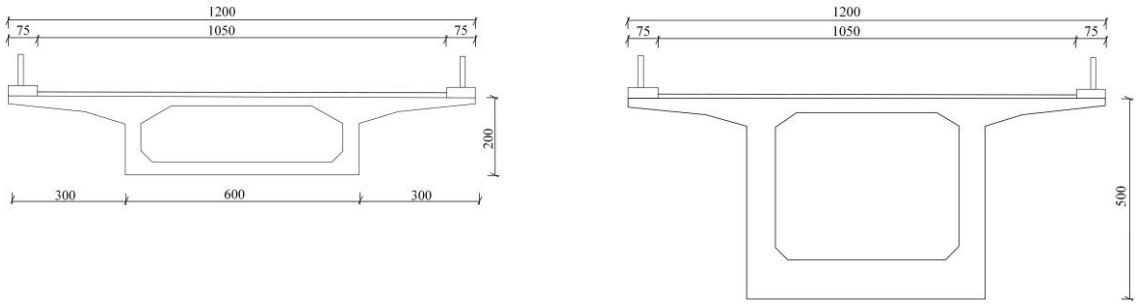

(a) Mid-span cross-section *(b) Pier support cross-section*

Fig. 2 - Cross-sectional views of box girder at mid-span and pier top (Unit: cm)

The T-beam rigid frame employs Grade 50 concrete with an elastic modulus of 3.41×10^5 MPa, and a standard tensile strength of 1860 MPa. The deformation of anchorages, steel strand retraction, and joint compression are 0.006 m per end. The friction coefficient between the prestressing tendons and the pipeline wall is taken as 0.25. Transverse prestressing tendons are also made of steel strands with a diameter of φ15.24, while vertical prestressing tendons utilize 75/100 high-strength finished threaded steel bars. The characteristic values for several key control sections of the bridge are shown in Table 1.

Tab.1 - Main control sections

Section Locatio	Section Number	Height (m)	Area (m²)	Sectional Bending Stiffness (kN·m²)
Top of Middle Pier	A-A	5.00	14.282	1.700×10^9
1/8 Section of Main Span	B-B	3.93	14.154	1.662×10^9
2/8 Section of Main Span	C-C	2.86	14.086	1.646×10^9
3/8 Section of Main Span	D-D	2.22	14.070	1.645×10^9
4/8 Section of Main Span	E-E	2.00	7.304	1.643×10^9

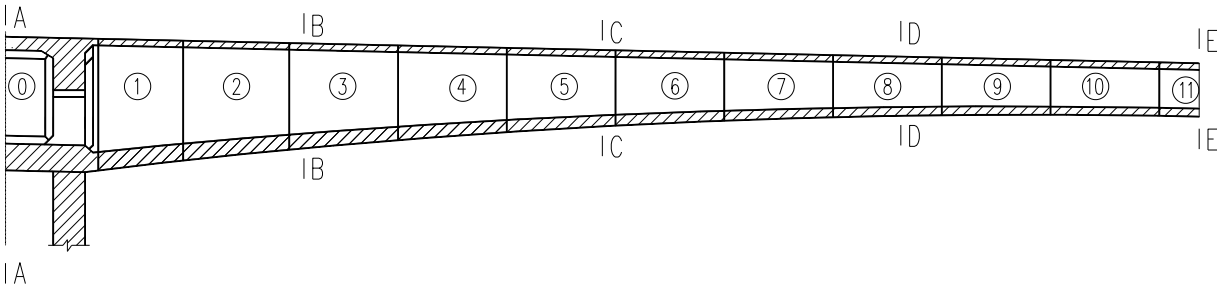

Fig. 3 - Main Control Sections

This continuous rigid frame bridge began operating in October 1997. During a general survey of the bridge in 2007, it was discovered that the main span had significant downward deflection, which was continuing to develop. Subsequently, a comprehensive inspection was conducted on the bridge. The inspection results revealed that the deflection values, strain values, and crack widths of the bridge exceeded the specifications and requirements, failing to meet the design load requirements for Highway-Super 20 vehicles. The safety reserve for load-bearing capacity was severely insufficient. To ensure the normal use of the bridge and the safety of traffic, reinforcement measures were proposed for the bridge, which should be carried out according to the load rating requirements of Highway-Class I as specified in the 2004 specifications. In November 2009, the reinforcement work of the bridge was completed. Static and dynamic load tests conducted on the bridge showed that it met the requirements of Highway-Class I, with deflection, strain, and cracks all within acceptable limits. Six years after the external prestressing reinforcement was implemented, a regular inspection and load test were conducted on the bridge.

The Impact of Internal Prestress Loss on Bridge Deflection

There has been a lack of systematic experimental research data on the impact of prestress on deflection, thus it is necessary to study the pattern of deflection as it varies with external prestress. When considering the influence of long-term deformation under short-term loading, the specific formula for solving the deflection value is:

$$\delta = \delta_0 + \beta \frac{\iint M dx dx}{(1+k_1)EI} N_y \qquad (1)$$

$$\Delta\delta = \beta \frac{\iint M dx dx}{(1+k_1)kEI} \Delta N_y \qquad (2)$$

In the formula:

β —represents the coefficient of influence of external prestress on deflection;

M — represents the bending moment generated by dead load;

δ0 —represents the deflection produced by dead load when there is no external prestress.

To study the impact of internal prestress loss on the downward deflection of bridges, simulations were conducted for longitudinal prestress losses of 10%, 15%, 20%, 25%, and 30%, respectively. The deflection values obtained were plotted in Figure 4.

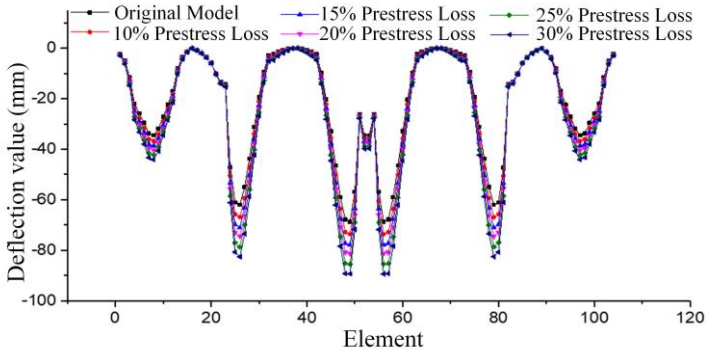

Fig. 4 - Comparison chart of deflections caused by different levels of internal prestress loss

As can be seen from Figure 4, with the increase in longitudinal prestress loss, the deflection values of each cross-sectional unit across the entire bridge increase significantly. Notably, the deflection values of the units near the mid-span of the bridge show larger changes, while the changes in other units are relatively small. To further illustrate this, the deflection differences between the original mid-span model and the models with 10%, 15%, 20%, 25%, and 30% longitudinal prestress loss are plotted in Figure 5.

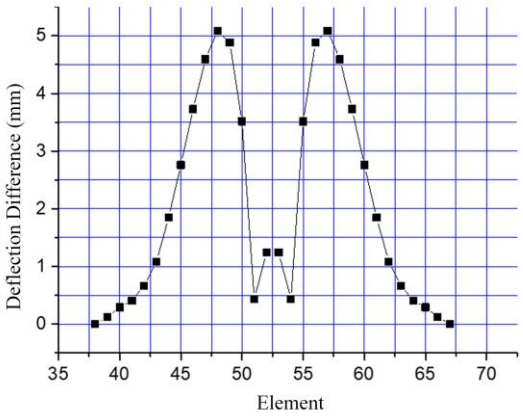

(a) 10% loss

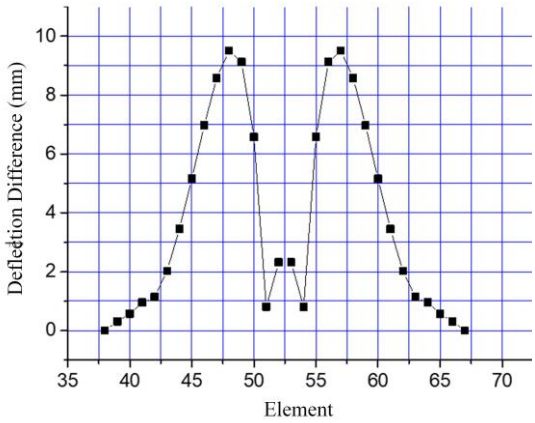

(b) 15% loss

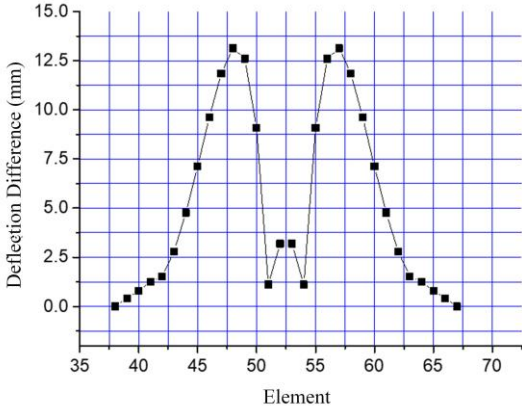

(c) 20% loss

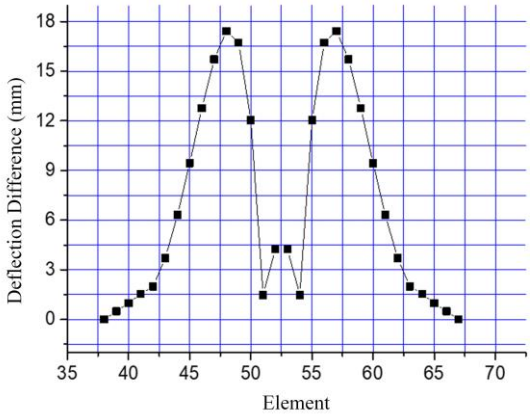

(d) 25% loss

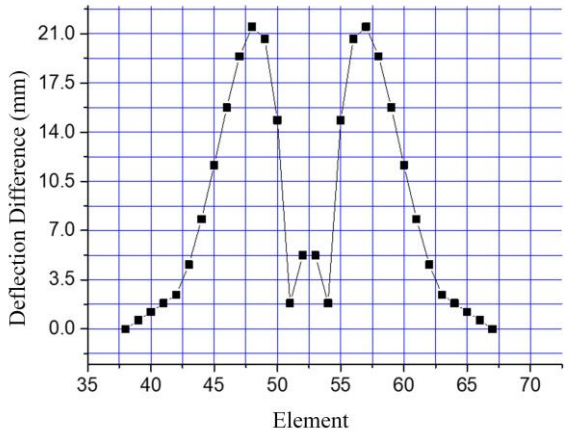

(f) 30% loss

Fig. 5 - Deflection differences between the original model and models with longitudinal prestress loss

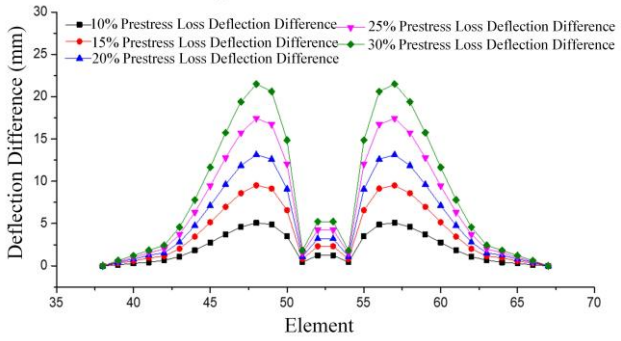

Fig. 6 - Comparison of deflection differences between the original model and models with 10%, 15%, 20%, 25%, and 30% longitudinal prestress loss

From Figures 5 and 6, it can be observed that as the longitudinal prestress loss increases, the deflection difference also increases. When the longitudinal prestress loss reaches 10%, the maximum reduction in deflection for units near the mid-span of the main bridge is 5.09mm. Furthermore, as seen in Figures 5 and 6, when the longitudinal prestress loss reaches 30%, the maximum decrease in deflection near the mid-span is 21.50 mm. In summary, the loss of longitudinal prestress is one of the most significant factors contributing to an increase in bridge deflection.

The Impact of Stiffness Reduction on Bridge Deflection

Stiffness represents the ability of a material or structure to resist deformation. For long-span continuous rigid-frame bridges, structural stiffness is particularly important. The reduction in stiffness can be influenced by various complex factors, and the main reasons for the overall structural stiffness decline are large-area cracking of webs and the appearance of transverse cracks in the mid-span area.

When a structure is subjected to loading, once the bending moment generated at a section reaches the cracking bending moment of that section, cracking will occur, leading to uneven changes in structural stiffness along the longitudinal direction of the bridge and rendering the structure out of its intended working condition. Therefore, the effective moment of inertia of the section should be used for calculations, as shown in Equation (3):

$$I_e = \left(\frac{M_{cr}}{M}\right)^3 I_{ucr} + \left[1 + \left(\frac{M_{cr}}{M}\right)\right] I_{cr} \le I_{ucr} \quad (3)$$

In the formula:

M—represents the bending moment generated by the structure under service loads.

M_{cr} —represents the bending moment at which the section cracks.

I_{ucr} —represents the converted inertia of the section before cracking.

I_{cr} represents the converted inertia of the section at the point of cracking.

To illustrate the change in bridge deflection as the amount of stiffness reduction increases, the deflection values resulting from stiffness reductions of 10%, 15%, 20%, 25%, 30%, and 35% have been plotted in Figure 7. The reduction in stiffness in the text is achieved by adjusting the elastic modulus of the cross-sectional material.

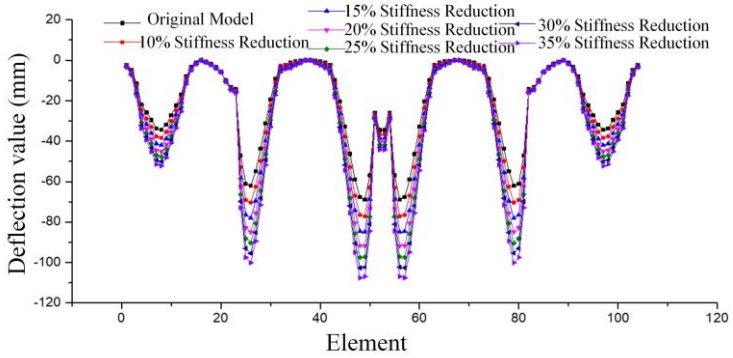

Fig. 7 - Comparison chart of deflections caused by different levels of stiffness reduction

As shown in the figure, the higher the degree of stiffness reduction, the larger the deflection values of each cross-sectional unit across the entire bridge. It is evident that the deflection values of the units near the mid-span of the bridge show significant changes, while the deflection values of the other units change very little and are almost unaffected. To more clearly understand the extent to which stiffness reduction affects deflection, the deflection differences between the original mid-span model and the models with reduced stiffness have been plotted in Figures 8 to 9.

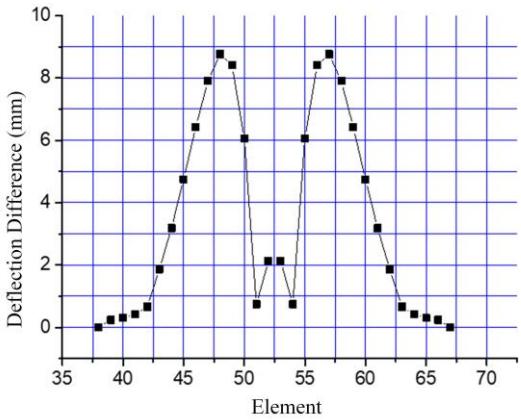

(a) 10% reduction in stiffness

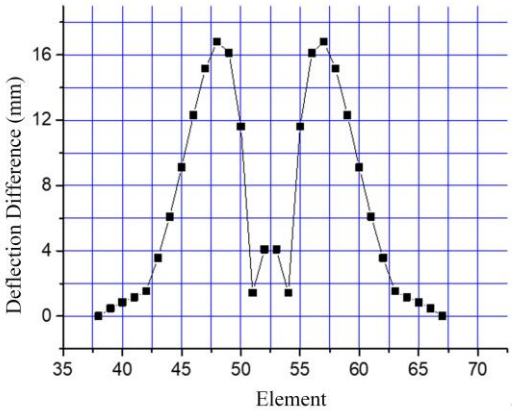

(b) 15% reduction in stiffness

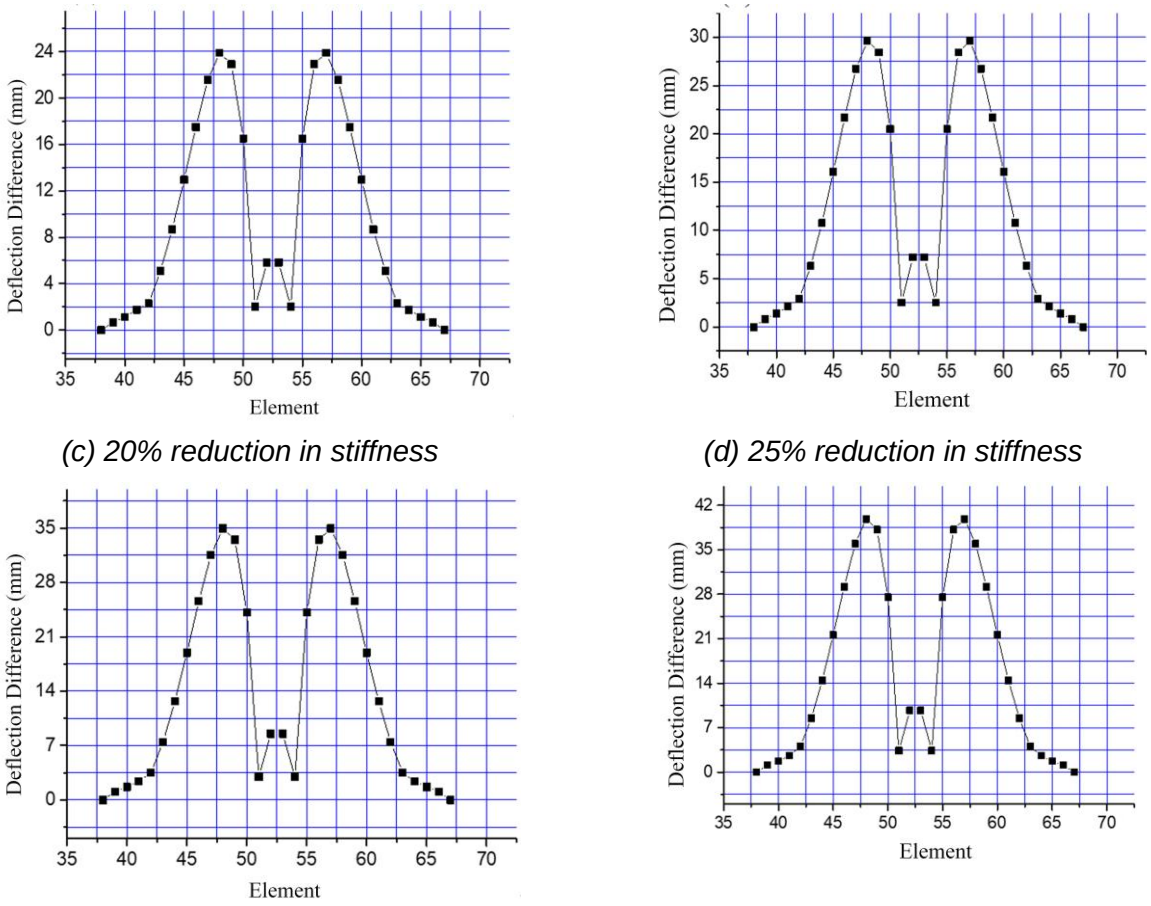

(c) 20% reduction in stiffness

(d) 25% reduction in stiffness

(e) 30% reduction in stiffness

(f) 35% reduction in stiffness

Fig.8 - Deflection difference between the original model and the model with stiffness reduction

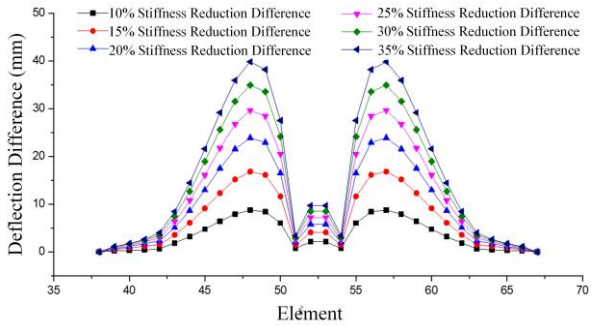

Fig. 9 - Comparison of deflection differences between the original model and models with 10%, 15%, 20%, 25%, 30%, and 35% stiffness reduction

From Figures 8 to 9, it can be observed that as the stiffness reduction increases, the deflection difference also increases. When the stiffness is reduced by 10%, the deflection difference plot shows that the maximum decrease in deflection near the mid-span is 8.76 mm. As the stiffness reduction further increases, the deflection continues to decline. Figure 9 shows that when the stiffness is reduced by 35%, the maximum decrease in deflection near the mid-span is 39.81 mm.

The impact on the maximum deflection of the mid-span, the secondary side-span, and the

primary side-span of the bridge under seven different operating conditions is shown in Figure 10.

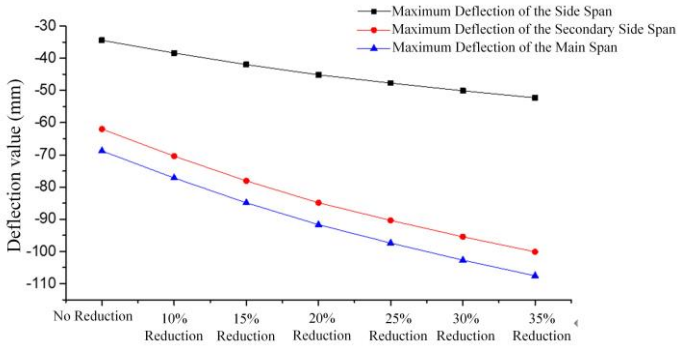

Fig.10- Comparison of maximum deflection values between the original model and models with different levels of stiffness reduction

From Figure 10, it can be seen that the maximum deflection of the side span is -34.43mm when there is no stiffness reduction. When the stiffness is reduced by 10%, 15%, 20%, 25%, 30%, and 35%, the maximum deflection of the side span increases by 11.40% (-3.93 mm), 21.89% (-7.53 mm), 31.10% (-10.71 mm), 38.59% (-13.29 mm), 45.50% (-15.66 mm), and 51.83% (-17.85 mm) respectively, compared to the case with no stiffness reduction. The maximum deflection of the secondary side span increases by 13.53% (-8.39 mm), 25.96% (-16.09 mm), 36.89% (-22.87 mm), 45.77% (-28.37 mm), 53.97% (-33.46 mm), and 61.48% (-38.11 mm) respectively. The maximum deflection of the mid-span increases by 12.22% (-8.40 mm), 23.45% (-16.12 mm), 33.32% (-22.91 mm), 41.62% (-28.62 mm), 49.34% (-33.93 mm), and 56.42% (-38.80 mm) respectively. In summary, stiffness reduction is one of the most important factors affecting the deflection of continuous rigid-frame bridges.

The impact of shrinkage and creep on bridge deflection

Currently, technology has not yet been able to accurately simulate the shrinkage and creep of concrete due to its significant dispersion. Therefore, we select the average relative humidity of the environment as an indicator to simulate the characteristics of shrinkage and creep. According to relevant specifications, when 40% < RH < 70%, we choose RH = 55%. When 70% < RH < 99%, we choose RH = 80%. Based on this requirement, we selected the change in bridge deflection values when RH is 80%, 70%, 55%, and 40%. Due to the space limitations of this article, only the deflection values for half of the main span are listed. The deflection differences between the deflection values under three operating conditions and the original model are shown in Figure 11.

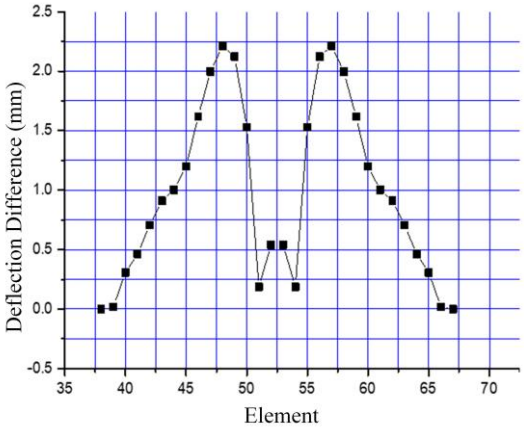

(a) Comparison between operating condition 1 and operating condition 2

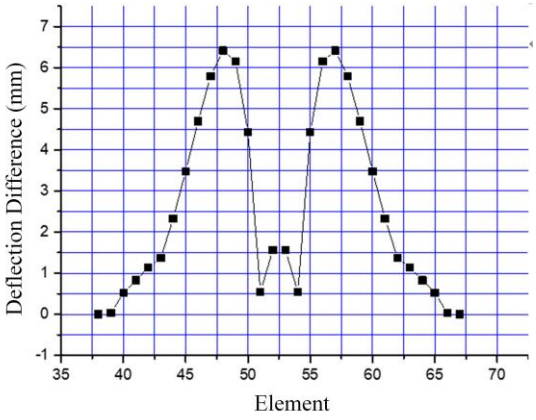

(b) Comparison between operating condition 1 and operating condition 3

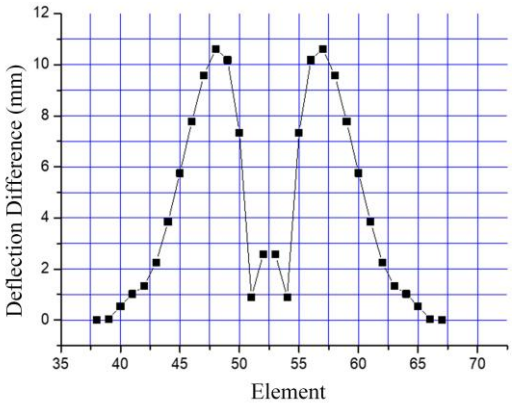

(c) Comparison between operating condition 1 and operating condition 4

Fig. 11- Deflection differences between various operating conditions

The overall deflection of the bridge under four different operating conditions as a function of the average relative humidity of the environment is shown in Figure 12.

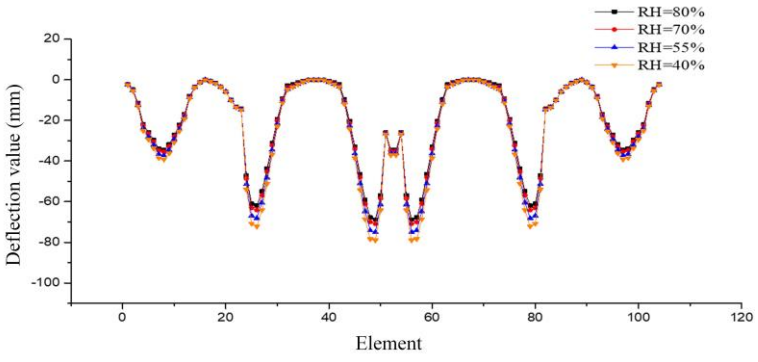

Fig.12- Comparison of deflections at RH=80%, RH=70%, RH=55%, and RH=40%

From Figures 11 and 12, it can be observed that the lower the average relative humidity (RH) of the environment, the greater the deflection values of each cross-sectional unit of the entire bridge. It is evident that the deflection values of the units near the mid-span of the bridge change significantly,

while the deflection values of the other units change very little and are almost unaffected by the average relative humidity of the environment. When the average relative humidity is RH=70%, the maximum deflection decreases by 2.21 mm compared to the original model's deflection value. Figure 12 shows that when the average relative humidity is RH=40%, the maximum decrease in deflection near the mid-span is 10.62 mm. The maximum deflection values of the mid-span cross-sections of each span of the bridge under the four operating conditions are shown in Figure 13.

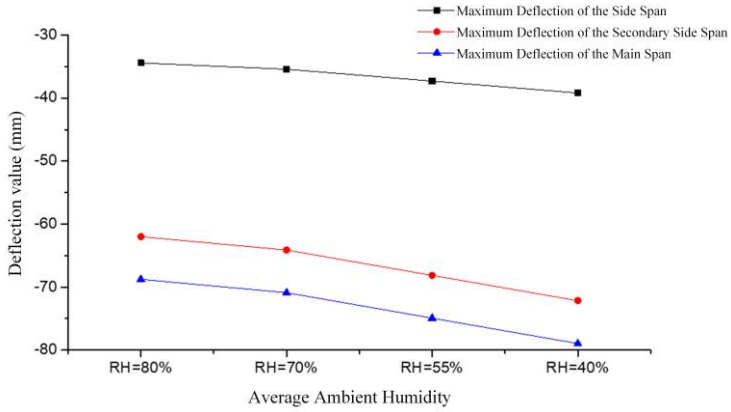

Fig.13 Comparison of deflections at RH=80%, RH=70%, RH=55%, and RH=40%

Table 2 shows the maximum deflection values of the mid-span, secondary side span, and side span under Operating Conditions 1 to 4.

Tab. 2 - Impact of shrinkage and creep on deflection

Calculation Scenarios	Calculated deflection values at specific locations（mm）		
	Maximum deflection of the side span	Maximum deflection of the secondary side span	Maximum deflection of the mid-span
RH=80%	-34.43	-61.99	-68.77
RH=70%	-35.42	-64.11	-70.89
RH=55%	-37.30	-68.13	-74.92
RH=40%	-39.19	-72.16	-78.95

From Figure 13 and Table 2, it can be seen that when the average relative humidity (RH) is 80%, the maximum deflection of the side span is -34.43 mm. When the RH is 70%, 55%, and 40%, respectively, the maximum deflections of the side span increase by 2.87% (-0.99 mm), 8.34% (-2.87 mm), and 13.83% (-4.76 mm) compared to when RH is 80%. Similarly, the maximum deflections of the secondary side span increase by 3.42% (-2.12 mm), 9.90% (-6.14 mm), and 16.41% (-10.17 mm), respectively, compared to when RH is 80%. The maximum deflections of the mid-span also increase by 3.08% (-2.12 mm), 8.94% (-6.15 mm), and 14.80% (-10.18 mm), respectively, under the same comparison. The analysis of these data indicates that shrinkage and creep is one of the factors affecting the deflection of continuous rigid frame bridges, but it is not the primary factor.

The impact of super-elevation on bridge deflection

During the construction of box girder bridges, the actual amount of concrete poured is often greater than the designed amount, a phenomenon known as concrete overfill in box girders.

Currently, there are no definitive and guiding research results regarding concrete overfill in box girders. Additionally, issues such as formwork bulging can occur during construction, making it difficult to control overfill. Although it is stipulated that overfill of no more than 5% is not considered significant, studying the issue of overfill still holds certain guiding significance.

Finally, we have identified four operating conditions to consider the extent to which deflection values are affected by concrete overfill:

Operating Condition 1: No overfill
Operating Condition 2: 5% overfill
Operating Condition 3: 6% overfill
Operating Condition 4: 7% overfill
Operating Condition 5: 8% overfill

Due to the limitations of this paper, only the deflection values for half of the main span are listed. The deflection values resulting from 5%, 6%, 7%, and 8% overfill are plotted in a graph to reflect the extent to which deflection values are affected by overfill. The specific changes are shown in Figure 14.

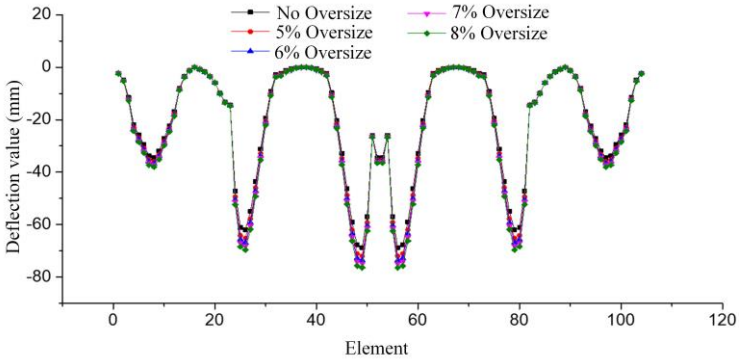

Fig.14 - Deflection values tesulting from structures with different amounts of concrete overfill

As can be seen from Figure 14, with the increase in the amount of concrete overfill, there is a tendency for the deflection of each section of the main girder to increase. However, when the proportion of overfill is the same, the degree of influence on each section varies. To reflect the pattern of change in deflection with increasing overfill, the differences in deflection between the original mid-span model and the models with 5%, 6%, 7%, and 8% overfill are plotted in Figures 15 to 16, respectively.

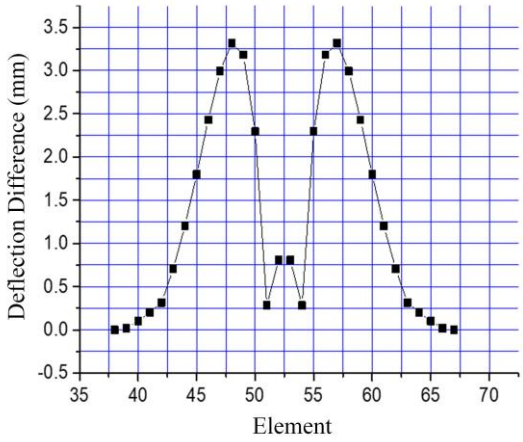

(a) 5% overfill

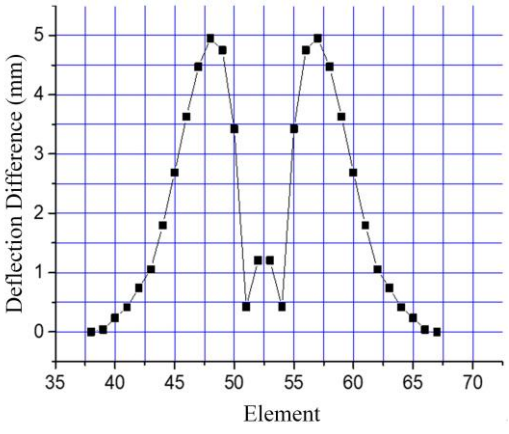

(b) 6% overfill

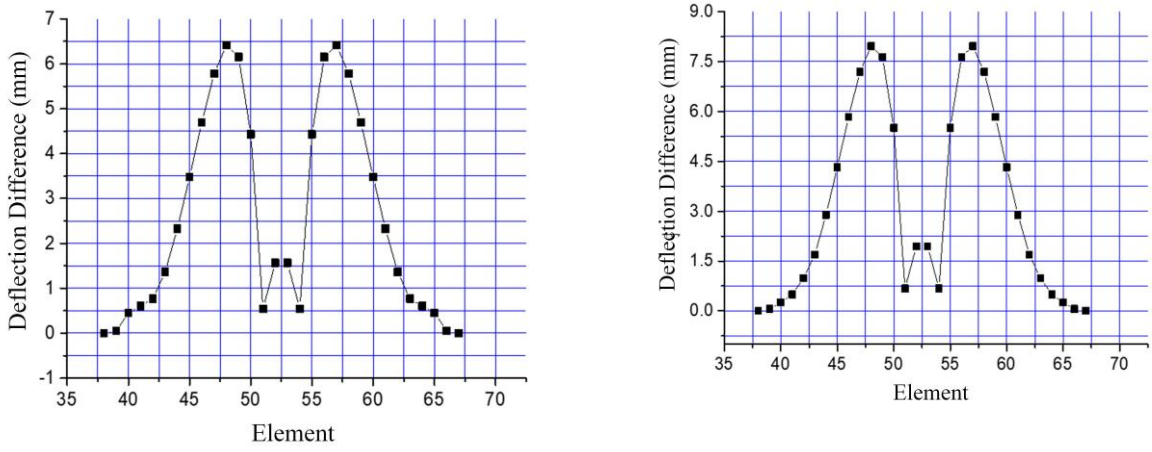

(c) 7% overfill *(d) 8% overfill*

Fig.15- Deflection Differences Between No Overfill and Various Amounts of Overfill

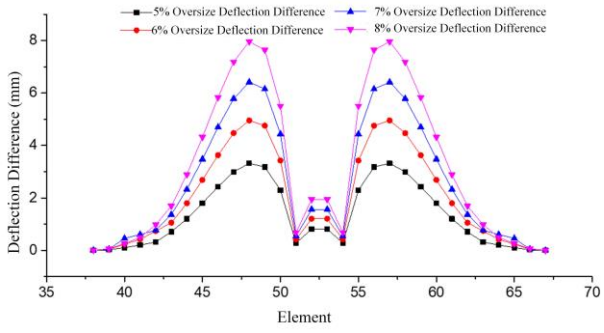

Fig.16- Deflection differences between the original model and models with 5%, 6%, 7%, and 8% overfill

From Figures 15 to 16, it can be observed that as the amount of concrete overfill increases, the deflection values of each cross-sectional unit of the entire bridge also increase, but the degree of change is relatively small, indicating that the impact of overfill on bridge deflection values is relatively minor. Furthermore, it is evident that the deflection values of units near the mid-span of the bridge change significantly, while the deflection values of other units change slightly. When there is 5% overfill, the maximum deflection difference observed from the deflection difference graph is 3.31 mm. However, as the amount of overfill increases, as shown in Figure 16, when there is 8% overfill, the maximum deflection difference reaches 7.96 mm. Therefore, although overfill can affect the downward deflection of the bridge mid-span, it is not the primary factor, and the impact of the amount of overfill is relatively small.

The Impact of Shear Deformation on Bridge Deflection

When calculating rigid frame bridges, due to their large slenderness ratio, the influence of shear deformation on the structure is often neglected. In some research analyses, a height-to-span ratio (H/L) of less than 1/5 is used as an indicator to determine whether to consider the impact of shear deformation on the structure. In continuous rigid frame bridges, the height-to-span ratio is far less than 1/5, but their main beams are box girder structures with thin webs that are significantly affected by shear forces. Furthermore, prestressing can eliminate most bending deformations but

has no effect on shear deformations, which amplifies the influence of shear deformation. Therefore, the impact of shear deformation should not be ignored.

Two operating conditions are selected for analysis:

Operating Condition 1: Shear deformation is considered.

Operating Condition 2: Shear deformation is not considered.

The impact of Operating Conditions 1 and 2 on the deflection after reinforcement is shown in Figure 17.

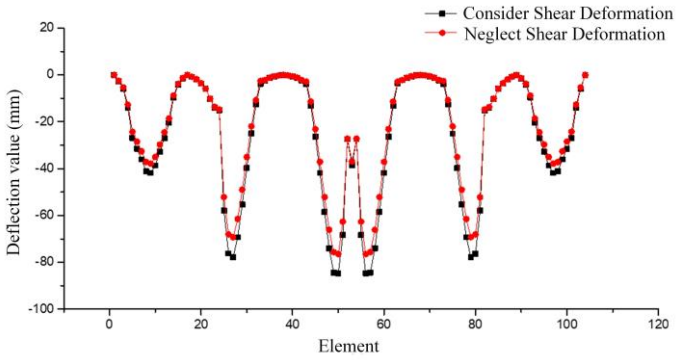

Fig.17 - Impact of shear deformation on deflection

From Figure 17, it can be observed that shear deformation has an impact on the deflection values of this continuous rigid frame bridge, with a significant influence on the units near the mid-span. To more clearly reflect the impact of shear deformation on deflection, the mid-span deflection difference is shown in Figure 18, and the deflection differences for each span are presented in Table 3.

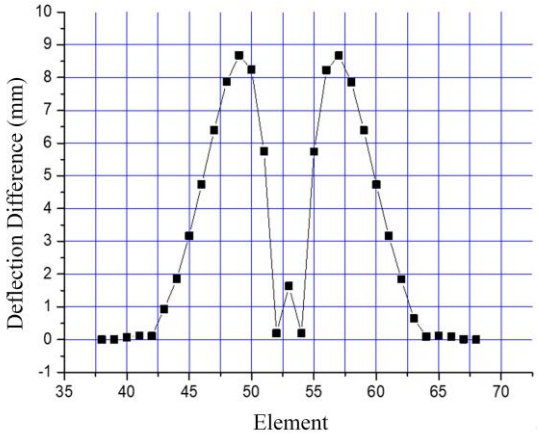

Fig.18 - Deflection difference between considering and not considering shear deformation in the mid-span

Tab.3 - Impact of considering shear deformation on deflection

Condition	Maximum Deflection（mm）		
	Maximum Deflection of the Side Span	Maximum Deflection of the Secondary Side Span	Maximum Deflection of the Middle Span
Under the condition of considering shear deformation	-41.87	-77.87	-84.68
Under the condition of not considering shear deformation	-37.88	-69.26	-76.44

From Table 3 and Figure 18, it can be observed that the deflection of the middle span considering shear deformation is 10.78% (8.24 mm) greater than that without considering shear deformation. Similarly, the deflection of the secondary side span considering shear deformation is 12.43% (8.61 mm) higher, and the deflection of the side span considering shear deformation is 10.53% (3.99 mm) more than that without considering shear deformation.

Based on the above analysis, it can be concluded that the height-to-span ratio (H/L) of less than 1/5 cannot be used as a sole criterion for neglecting shear deformation. For this bridge, with a height-to-span ratio ranging from 1/18 to 1/45, which is much smaller than 1/5, the deflection considering shear deformation is still more than 10% greater than that without considering it. Therefore, the impact of shear deformation cannot be ignored.

Impact of External Prestressing Loss on Bridge Deflection

To investigate the impact of loss in external prestressing tendons on the deflection of continuous rigid frame bridges, this subsection employs a method of reducing the tension control force to simulate a certain level of reduction in external prestressing tendons. Five operating conditions are considered: no reduction, 5% reduction, 10% reduction, 15% reduction, and 20% reduction. By calculating the bridge under these five conditions, the deflection values of the entire bridge are obtained for each scenario. The specific operating conditions are defined as follows:

Operating Condition 1: No reduction.

Operating Condition 2: 5% reduction in external prestressing tendons.

Operating Condition 3: 10% reduction in external prestressing tendons.

Operating Condition 4: 15% reduction in external prestressing tendons.

Operating Condition 5: 20% reduction in external prestressing tendons.

Due to space limitations in this document, only the deflection values for half of the main span are listed. The deflection differences between each operating condition and the original model are shown in Figures 19 to 20. The prestress loss in the text is achieved by adjusting the tension stress of the prestressed steel strands. The prestress loss is realized by reducing the tension stress of the steel strands.

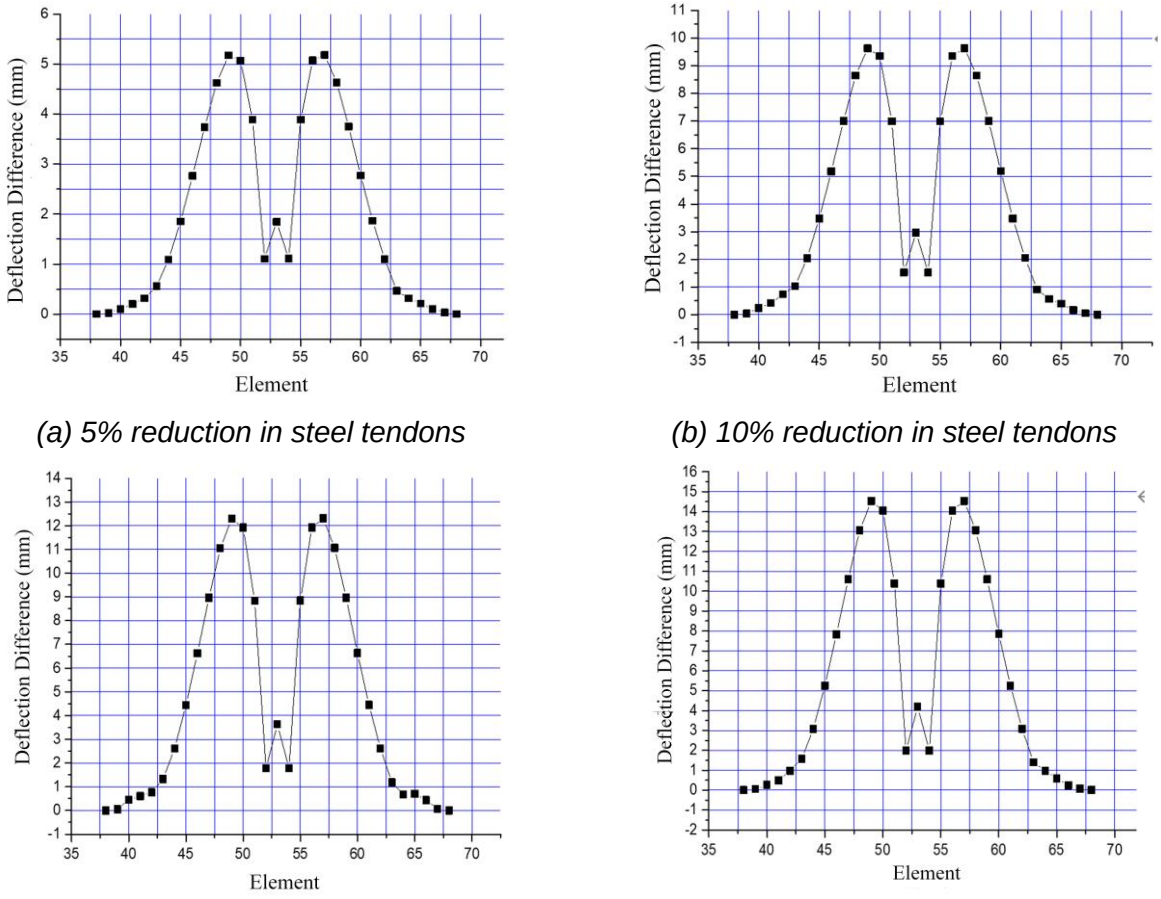

(a) 5% reduction in steel tendons

(b) 10% reduction in steel tendons

(c) 15% reduction in steel tendons

(d) 20% reduction in steel tendons

Fig.19- Deflection difference between the original model and different levels of steel tendon reduction

The overall deflection of the bridge under the five operating conditions as it varies with the reduction of external prestressing is shown in Figure 20.

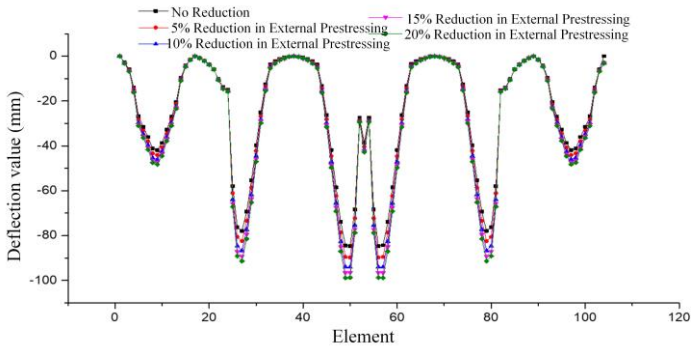

Fig.20- Comparison of deflections between the original model and models with 5%, 10%, 15%, and 20% reduction in steel tendons

From Figures 19 to 20, it can be observed that as the loss of external prestressing increases, the deflection values of each cross-sectional unit across the entire bridge also increase. Notably, the

deflection values of the units near the mid-span of the bridge show significant changes, while the deflection values of the other units remain almost unaffected by the loss. The deflection difference diagrams indicate that when the external prestressing loss is 5%, the maximum decrease in deflection near the mid-span is 5.07 mm. Figure 3-36 further shows that when the external prestressing loss reaches 20%, the maximum decrease in deflection near the mid-span is 14.06 mm.

The maximum deflection values at the mid-span sections of each span of the bridge under the five operating conditions are shown in Figure 21. The maximum deflection values at the mid-span sections of the entire bridge under Operating Conditions 1 to 5 are listed in Table 4.

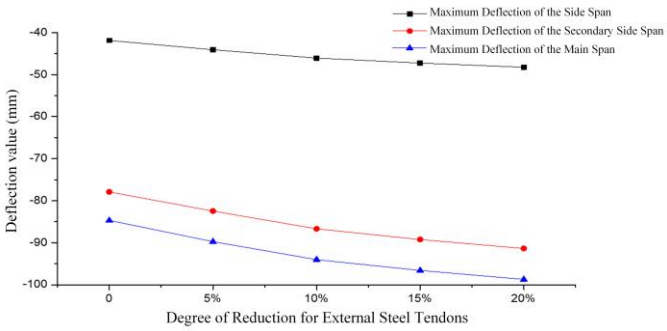

Fig.21 - Comparison of deflections between the original model and models with 5%, 10%, 15%, and 20% reduction in steel tendons

Tab. 4 - Impact of external prestressing reduction on bridge deflection values

Operating Conditions:	Maximum Deflection Value（mm）		
	Maximum value of side span	Maximum value of secondary side span	Maximum value of middle span
Operating Condition 1: No Reduction	-41.87	-77.90	-84.68
Operating Condition 2: 5% Reduction	-44.07	-82.46	-89.75
Operating Condition 3: 10% Reduction	-46.06	-86.70	-94.03
Operating Condition 4: 15% Reduction	-47.25	-89.25	-96.60
Operating Condition 5: 20% Reduction	-48.25	-91.37	-98.74

From Figure 21 and Table 4, we can observe that the maximum deflection of the side span in the original bridge model without any loss is -41.87 mm. When the external prestressing loss is 5%, 10%, 15%, and 20% respectively, the maximum deflection of the side span increases by 5.25% (-2.2 mm), 10.00% (-4.19 mm), 12.85% (-5.38 mm), and 15.24% (-6.38 mm) compared to the case with no reduction. Similarly, the maximum deflection of the secondary side span increases by 5.85% (-4.56 mm), 11.30% (-8.80 mm), 14.57% (-11.35 mm), and 17.29% (-13.47 mm) respectively. For the middle span, the maximum deflection increases by 5.99% (-5.07 mm), 11.04% (-9.35 mm), 14.08% (-11.92 mm), and 16.60% (-14.06 mm) respectively compared to the no-reduction case. The analysis of these data indicates that the deflection of continuous rigid frame bridges is directly proportional to

the degree of external prestressing reduction, which is a major factor affecting the reinforced continuous rigid frame bridges.

Impact of Overload Under Operational Live Load on Bridge Deflection

The bridge is located at a strategic traffic hub, and most of the passing vehicles are heavily loaded or overloaded, with maximum vehicle tonnage far exceeding the live load limits allowed by the specifications. Therefore, based on the actual situation of the bridge, an analysis of the impact of live load overload on the deflection values of the bridge is conducted. This analysis is divided into five operating conditions:

Operating Condition 1: Original Model
Operating Condition 2: Overload by 25%
Operating Condition 3: Overload by 50%
Operating Condition 4: Overload by 75%
Operating Condition 5: Overload by 100%

The impact of simulated overload on the deflection values of the bridge is shown in Figure 22.

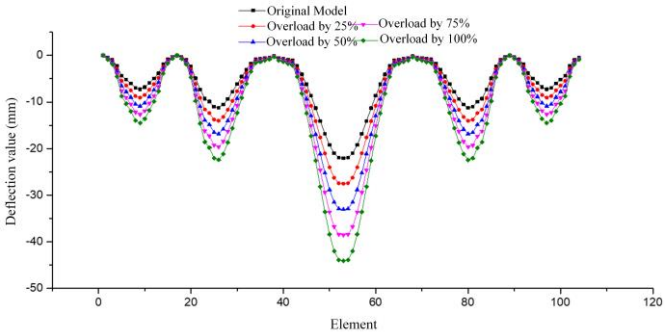

Fig. 22 - Deflection values of each bridge unit caused by different live load overloads

From Figure 22, it can be observed that as the live load overload increases, the deflection values of each cross-sectional unit across the entire bridge also increase. Notably, the deflection values of the units near the mid-span of the bridge show significant changes and are greatly affected by the live load overload, while the deflection values of the other units are less affected. The differences in deflection values caused by overloads of 25%, 50%, 75%, and 100% compared to the no-overload condition are shown in Figure 23.

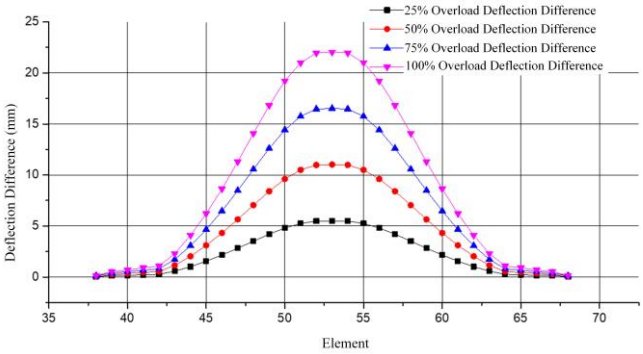

Fig.23 - Deflection differences between each unit of the main span due to overload and the original model

As can be seen from Figure 23, with the increase in overload, the deflection of each cross-

section gradually increases. When the load exceeds the design load by 25%, 50%, 75%, and 100%, the maximum deflection differences between the mid-span and the original model are 5.51 mm, 11.02 mm, 16.52 mm, and 22.03 mm, respectively. This indicates that overload has a significant impact on the deflection values of bridge cross-sections, and overload is an important factor affecting the downward deflection of the mid-span of reinforced bridges.

CONCLUSIONS

Using simulation analysis and calculation methods, the impact of various parameters on the deflection of a continuous rigid frame bridge was analyzed. The main parameters included: internal prestressing loss, stiffness reduction, shrinkage and creep, over-sizing, shear deformation, external prestressing loss, and overload. The research results of this paper have significant research significance and practical value for the reinforcement design of prestressed continuous rigid frame bridges. The following conclusions were obtained:

(1) Internal prestressing loss, stiffness reduction, shrinkage and creep, over-sizing, shear deformation, external prestressing loss, and overload all contribute to the downward deflection of the mid-span, but each factor has a different degree of influence.

(2) When comparing all factors comprehensively, stiffness reduction is the largest contributor to the downward deflection of the mid-span. For reinforced bridges, external prestressing loss and overload are the most significant factors. When the stiffness is reduced by 10%, the deflection difference plot shows that the maximum decrease in deflection near the mid-span is 8.76mm. When the external prestressing loss is 5% and 15% respectively, the maximum deflection of the side span increases by 5.25% (-2.2 mm) and 12.85% (-5.38 mm) compared to the case with no reduction.

(3) In the calculation of continuous rigid frame bridges, shear deformation cannot be ignored. It can be observed that the deflection of the middle span considering shear deformation is 10.78% (8.24 mm) greater than that without considering shear deformation.

REFERNCES

[1] Wang Q, Xian J, Xiao J., 2023. Intelligent Safety Assessment Method for Demolition Construction of Closure Segment of Long-span Continuous Rigid Frame Bridges. Advances in Bridge Engineering, vol. 4, no. 1, p. 9. ISSN 2662-5407, https://doi.org/10.1186/s43251-023-00088-z

[2] Hao X W, Duan R F, Chi D Y., 2013. Stress Analysis of Closure Process of Continuous Rigid Frame Bridge. Applied Mechanics and Materials, vol. 303, p. 2919-2923. https://doi.org/10.4028/www.scientific.net/AMM.303-306.2919

[3] Xin Y, Zhang J, Han X D., 2014. Research on Ultimate Load of Highway Prestressed Concrete U-Shaped Continuous Rigid Frame Bridge Based on Nonlinear Finite Method. Applied Mechanics and Materials, vol. 501, p. 1398-1402. https://doi.org/10.4028/www.scientific.net/AMM.501-504.1398

[4] Yang S, Hong Y, Pu Q., 2024. Mechanical Behaviour of Steel–concrete Joints in Railway Rigid Frame-continuous Composite System Bridge. Journal of Constructional Steel Research, vol. 222, p. 108946. ISSN 0143-974X, https://doi.org/10.1016/j.jcsr.2024.108946

[5] Shan A., 2015. Analytical Research on Deformation Monitoring of Large Span Continuous Rigid Frame Bridge during Operation. Engineering, vol. 7, no. 08, p. 477. ISSN 2095-8099, http://creativecommons.org/licenses/by/4.0/

[6] Ding Y, Xiang Z, Li Y., 2020. A Practical and Safe Optimization Method for Temporary Cable Layout on the Upper Beam of Beam-arch Composite Rigid Frame Bridge. International Journal of Safety and Security Engineering, vol. 10, no. 1, p. 89-95. ISSN 2041-9031, https://doi.org/10.18280/ijsse.100112

[7] Zhang W, Wang Z L, Tian S Z., 2012. FEM Study on Shear Stiffness of Sloping Segmental Joints in Cantilever Casting Concrete Bridges. Applied Mechanics and Materials, vol. 178, p. 2277-2280. https://doi.org/10.4028/www.scientific.net/AMM.178-181.2277

[8] Zhang K, Qi T, Li D., 2021. Load Testing and Health Monitoring of Monolithic Bridges with Innovative Reinforcement. International Journal of Structural Integrity, vol. 12, no. 6,p. 904-921. ISSN 1757-9864, https://doi.org/10.1108/IJSI-11-2020-0103

[9] Seo J H, VanTyne C J, Moon Y H., 2016. Prediction of Turn Down Warping During Hot Plate Rolling Based on A Gaussian Function. International Journal of Material Forming, vol. 9, p. 705-713. ISSN 1960-6206, https://doi.org/10.1007/s12289-015-1261-8

[10] Chen D, Xu Z, Qiu Y., 2021. Analysis of Influence Factors on Line Shape of High-speed Railway Beam-arch Combination Bridge. Insight-Civil Engineering, vol. 4, no. 1, p. 311-311. ISSN 2630-4716, https://doi.org/10.18282/ice.v3i1.311

[11] Niu Z, Zhang Z, Liu Z., 2023. Influence of Adjacent Deep Foundation Pit Construction on Main Beams of PC Continuous Box Girder Bridge. Academic Journal of Architecture and Geotechnical Engineering, vol. 5, no. 6, p. 26-28. ISSN 2663-1563, https://doi.org/10.25236/AJAGE.2023.050606

[12] Cao G, Shen J, Yang L., 2024. Experimental and Modeling Study on Long-Term Deformation of Three-Span Prestressed Concrete Continuous Box-Girder Bridge Model after Cracking. Journal of Bridge Engineering, vol. 29, no. 10, p. 04024073. ISSN 1084-0702, https://doi.org/10.1061/JBENF2.BEENG-6725

[13] Jiang L, Zheng L, Feng Y., 2020. Mapping the Relationship Between the Structural Deformation of A Simply Supported Beam Bridge and Rail Deformation in High-speed Railways. Proceedings of the Institution of Mechanical Engineers, Part F: Journal of Rail and Rapid Transit, vol. 234, no. 10, p. 1081-1092. ISSN 0954-4097, https://doi.org/10.1177/0954409719880668

[14] Pi C, You G, Chen Y., 2022. Research on Intelligent Integrated Installation Process and Equipment of Prefabricated Bridges. 2nd International Conference on Internet of Things and Smart City (IoTSC 2022). SPIE, vol. 12249, p. 983-996.

[15] Sun Y, Xu D, Zhu H., 2022. Complete Stress Indicator System for the Design of Concrete Box-Girder Bridges. Structures. vol. 38, p. 536-552. ISSN 2352-0124, https://doi.org/10.1016/j.istruc.2022.02.026

[16] Busfield M E, Le Heron D P., 2014. Sequencing the Sturtian Icehouse: Dynamic Ice Behaviour in South Australia. Journal of the Geological Society, vol. 171, no. 3, p. 443-456. ISSN 0016-7649, https://doi.org/10.1144/jgs2013-06

[17] Zhong X, Chen Z, Liu J., 2022. Experimental Research on the In-plane Performance of Discontinuous Modular Diaphragms. Thin-Walled Structures, vol. 173, p. 108905. ISSN 0263-8231, https://doi.org/10.1016/j.tws.2022.108905

[18] Wu Y, Deng Y, Liu X., 2025. Drop Hammer iMPact Tests of Airport Pavement Slabs Composed of Modified Rubber Aggregate Concrete. Construction and Building Materials, vol. 458, p. 139519. ISSN 0950-0618, https://doi.org/10.1016/j.conbuildmat.2024.139519

[19] Floyd M, King R, Paradissis D., 2023. Variations in Coupling and Deformation Along the Hellenic Subduction Zone. Turkish Journal of Earth Sciences, vol. 32, no. 3, p. 262-274. ISSN 1303-619X, https://journals.tubitak.gov.tr/earth/vol32/iss3/3

[20] Sun Y, Dai S, Xu D., 2020. New Extended Grillage Methods for the Practical and Precise Modeling of Concrete Box-girder Bridges. Advances in Structural Engineering, vol. 23, no. 6, p. 1179-1194. ISSN 1369-4332, https://doi.org/10.1177/1369433219891559